

Scaling of the Euler Characteristic, Surface Area, and Curvatures in the Phase Separating or Ordering Systems

Marcin Fiałkowski,¹ Aleksij Aksimentiev,² and Robert Hołyst^{1,3}

¹*Institute of Physical Chemistry PAS and College of Science, Department III, Kasprzaka 44/52, 01224 Warsaw, Poland*

²*Material Science Laboratory, Mitsui Chemicals, Inc., 1190 Kasama-cho, Sakae-ku, 247-8567 Yokohama, Japan*

³*Labo de Physique, Ecole Normale Supérieure de Lyon, 46 allée d'Italie, 69364 Lyon, cedex 07, France*

(Received 30 May 2000)

We present robust scaling laws for the Euler characteristic and curvatures applicable to any symmetric system undergoing phase separating or ordering kinetics. We apply it to the phase ordering in a system of the nonconserved scalar order parameter and find three scaling regimes. The appearance of the preferred nonzero curvature of an interface separating \pm domains marks the crossover to the late stage regime characterized by the Lifshitz-Cahn-Allen scaling.

DOI: 10.1103/PhysRevLett.86.240

PACS numbers: 64.60.Cn, 68.55.Jk, 75.40.Gb, 75.40.Mg

Surfaces are ubiquitous in nature since they accompany almost every phase transition (with some exceptions, e.g., Kosterlitz-Thouless phase transition). If we quench a uniform system into the thermodynamically unstable region in the phase diagram we observe the formation of domains [1–4] in this system. The domains coarsen in time and their dynamics depends on the local mean curvature of the interface between them [1,5]. Here we show that the curvature distribution and the Euler characteristic of these interfaces give a deep insight into the process of phase ordering kinetics.

The systems undergoing phase transitions often exhibit scaling phenomena, i.e., a morphological pattern of the domains at earlier times looks statistically similar to a pattern at later times apart from the global change of scale implied by the growth of $L(t)$ —the typical size of the domains. Quantitatively it means, for example, that the correlation function of the order parameter (density, concentration, magnetization, etc.) $g(\mathbf{r}, t) = g[\mathbf{r}/L(t)]$, where $L(t) \sim t^n$ with n different for different universality classes [1,6]. Assuming the scaling hypothesis we can derive all the scaling laws for different morphological measures such as the Euler characteristic, $\chi(t)$, surface area, $S(t)$, the distribution of the mean, $P_H(H, t)$, and the Gaussian, $P_K(K, t)$, curvatures. We find

$$\chi(t) \sim L(t)^{-d}, \quad (1)$$

$$S(t) \sim L(t)^{-1}, \quad (2)$$

$$P_H(H, t) = P_H^*[HL(t)]/L(t), \quad (3)$$

$$P_K(K, t) = P_K^*[KL(t)^{(d-1)}]/L(t)^{(d-1)}, \quad (4)$$

where d is the dimensionality of the system. The first law follows from the Gauss-Bonnet theorem, $\chi = \gamma \int dS K$, where $\int dS$ denotes the integral over the surface and γ is twice the inverse of the volume of a $(d-1)$ -dimensional sphere of radius 1 (for $d=3$, $\gamma = \frac{1}{2\pi}$). Since $K \sim L(t)^{-d+1}$ and $S \sim L(t)^{-1}$ we find scaling (1). The scaling law (2) follows from the congruency of the

domains [7]. In $d=2$ scalings (3) and (4) are equivalent. Despite the fact that such obvious tests for the scaling hypothesis exist they have not been checked in computer simulations even for the simplest system exhibiting phase ordering kinetics, i.e., the three-dimensional (3D) system of the scalar nonconserved order parameter. Here we fill this apparent gap and also point out that these tests are robust, i.e., apply to any system exhibiting phase ordering or separation.

The model.—The evolution of the system of the scalar nonconserved order parameter following a quench from the temperature $T = \infty$ to $T = 0$ follows the time dependent Ginzburg-Landau (TDGL) equation [1,5,6,8,9]: $\partial \phi(\mathbf{r}, t)/\partial t = -\delta F[\phi]/\delta \phi$, where the Ginzburg-Landau free energy functional is given by

$$F[\phi] = \int d\mathbf{r} \left(\frac{1}{2} |\nabla \phi(\mathbf{r})|^2 + f(\phi(\mathbf{r})) \right), \quad (5)$$

and the bulk free energy $f(\phi) = -\phi^2/2 + \phi^4/4$. The equations have been solved on the cubic lattice of sizes ranging from 40^3 to 100^3 . All the quantities computed in the simulations have been averaged over 150 runs. A simple Euler integration scheme with time step $\Delta t = 0.05$ and mesh size $\Delta x = 1$ has been used. The initial conditions have been chosen from the uniform distribution of field ϕ with zero mean. In order to check the results against numerical artifacts we have varied the mesh size between $\Delta x = 0.5$ and 2 and also used 6, 18, and 26 point approximations for the Laplacian with no apparent changes in the obtained results. Additionally we have studied a 2D system of size 1024×1024 .

The method of analysis.—Every time step we determine the position of the interface separating the \pm domains. The interface given by the equation $\phi(\mathbf{r}) = 0$ is located (on the cubic lattice) by the linear interpolation of field ϕ between the lattice points. We find that after the initial transient time with many separated interfaces we get into the regime where there is a single surface in the system separating the $\phi > 0$ domain from the $\phi < 0$ domain. The \pm domains percolate and the system is bicontinuous. The surface

is triangulated: The surface area is computed as the area of all the triangles covering the surface, and the Euler formula has been used to compute χ , i.e., $\chi = F + V - E$, where F is the number of faces of the triangles, V is the number of vertices of the triangles, and E is the number of edges. The computation of the curvatures from the bulk field ϕ using the standard differential geometry [10,11] has proven to be inaccurate. Therefore we have used the very accurate Descartes formula which is described below. For each vertex on our triangulated surface we can define an angle deficit by $T_i = 2\pi - \sum_{j=1}^m \alpha_i^j$, where m is the number of triangles which meet at the i th vertex, and α_i^j is the angle between the two edges of the j th triangle at this vertex. The Gaussian curvature at the i th vertex is given by $K_i \approx T_i/S_i$, where S_i is $\frac{1}{3}$ of the area of the triangles. In order to check this formula we have used the Gauss-Bonnet theorem relating K and χ . In our simulations the relative error is less than 10^{-6} ; additionally we have tested it on the minimal surfaces [10,11] with similar accuracy. The mean curvature, H_i , at the i th vertex has been computed from the following formula: $H_i S_i = \frac{1}{4} \sum_{j=1}^m l_i^j \theta_i^j$, where l_i^j is the length of the edge of the j th triangle, and θ_i^j is the angle between the adjacent triangles j and $j + 1$. We have determined the distribution of the Gaussian and mean curvatures for the surface during the ordering transition. We have also determined the equal time correlation function: $g(\mathbf{r}, t) = \langle \text{sgn}(\phi(\mathbf{r}, t)) \text{sgn}(\phi(0, t)) \rangle$ for which an approximate, analytical formula exists, given by Ohta, Jasnow, and Kawasaki [12]:

$$g(\mathbf{r}, t) = \frac{2}{\pi} \arcsin\{\exp[-\mathbf{r}^2/L(t)^2]\}. \quad (6)$$

Equation (6) has been used to derive the exponent n . This equation and some other slightly inferior approximations [13,14] have been shown to work well [15–19], despite certain problems with the assumptions underlying these approximations [16,17].

The results.—In Fig. 1 we show $\chi(t)$, $S(t)$, $L(t)$ [obtained from Eq. (6)], and $\langle |\phi| \rangle$ as a function of time for three system sizes: 50^3 , 80^3 , and 100^3 . As we can see there is a clear change in the slope of $\ln\chi$ indicating the change of the scaling regime. In the early regime the exponent for χ is $-\frac{3}{2}(-1.53 \pm 0.05)$ and in the intermediate regime $-1(-1.04 \pm 0.05)$. For $S(t)$ we find the exponent $-\frac{1}{2}(-0.51 \pm 0.01)$ in the first regime and $-\frac{2}{5}(-0.40 \pm 0.01)$ in the second regime. The crossover time does not depend on the size of the system and from the plot of $\ln\langle |\phi| \rangle$ we find that it corresponds to the saturation of the order parameter, (± 1), inside the domains. In Fig. 2 the histograms for the mean curvature are shown for two scaling regimes. As we can see from this figure in both regimes $P_H(H, t) = P_H^*[HL(t)]/L(t)$, but in the early regime $n = 0.50 \pm 0.01$ and in the intermediate regime $n = 0.41 \pm 0.02$ (Fig. 1). $P_H(H, t)$ is peaked at $H = 0$. We find in the early regime $P_K(K, t) = P_K^*[KL(t)]/L(t)$, but in the intermediate $P_K(K, t) = P_K^*(Kt^{3/5})/t^{3/5}$. The average Gaussian curvature is negative. As we can see the scaling laws [(1),(4)] do not hold in the intermediate regime. We have additionally analyzed the scaling of the principal curvatures obtained from the

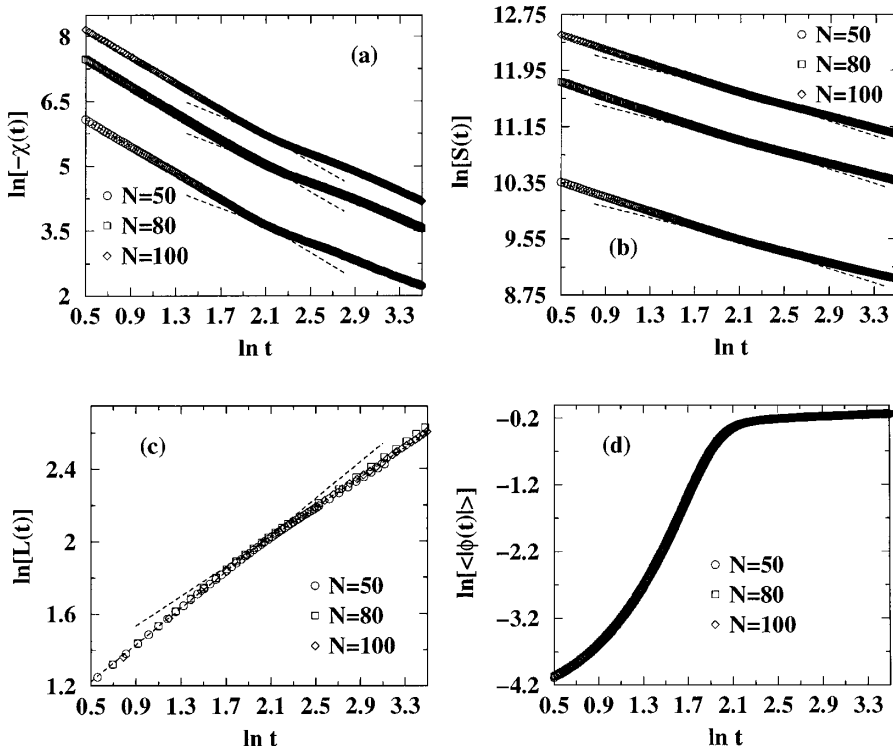


FIG. 1. The Euler characteristic χ (a), surface area S (b), characteristic size of the domain L (c), and the order parameter inside the domains $\langle |\phi| \rangle$ (d) as a function of time, t . The symbols correspond to system sizes $N = 50$ (\circ), 80 (\square), and 100 (\diamond). From the \ln - \ln plot we find the exponents $-\frac{3}{2}$ and -1 for $\chi(t)$, $-\frac{1}{2}$ and $-\frac{2}{5}$ for $S(t)$, and $\frac{1}{2}$ and $\frac{2}{5}$ for $L(t)$. The dashed lines show the fits in the two scaling regimes. The crossover time, $\ln t_{cr} \approx 2.1$, is marked by the saturation of the order parameter inside the domains as is evident from the plot (d).

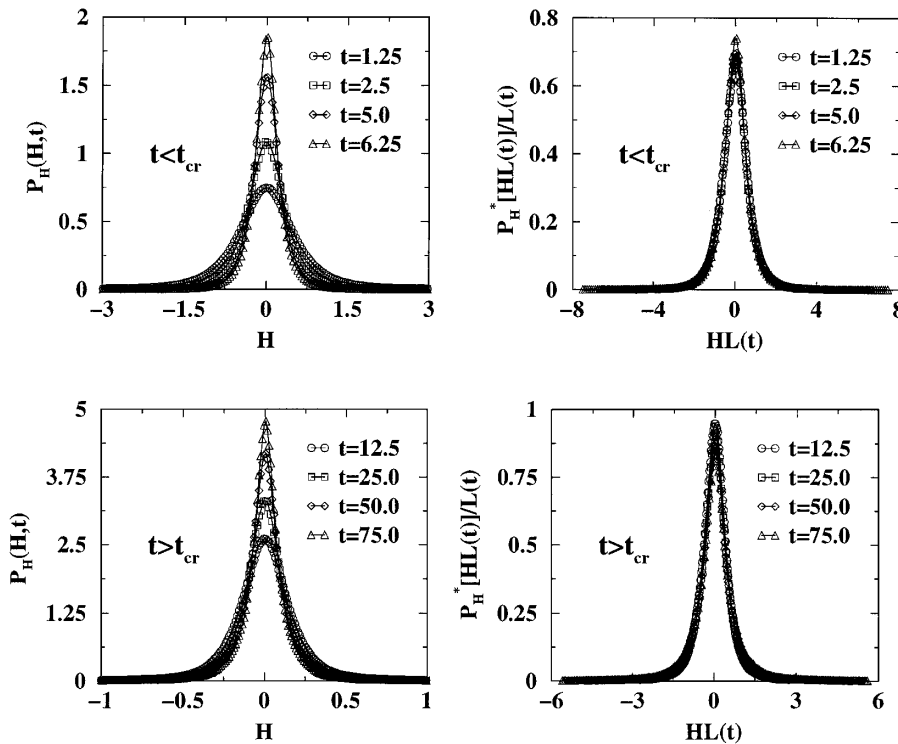


FIG. 2. The histograms of the mean curvature for different times shown together with the rescaled histograms. In both regimes (shown in Fig. 1) we find $P_H(H, t) = P_H^*[HL(t)]/L(t)$, with $L(t) = t^{1/2}$ for $t < t_{cr}$ and $L(t) = t^{2/5}$ for $t > t_{cr}$. The distributions P_H are normalized as $\int P_H(H, t) dH = 1$; the curvature H is given in dimensionless units. The system size is $50 \times 50 \times 50$.

equations $H = (1/R_1 + 1/R_2)/2$ and $K = 1/(R_1 R_2)$ and found that $\langle 1/R_1 \rangle = 1/S \int dS/R_1 \sim -\langle 1/R_2 \rangle = -1/S \int dS/R_2 \sim 1/L(t)$ in the early regime and $\sim t^{-1/10}$ in the intermediate regime. Additionally we have determined $\langle K \rangle / \sqrt{\langle 1/R_1^2 \rangle \langle 1/R_2^2 \rangle} \sim \text{const}$ in the early regime and $\sim t^{-1/2}$ in the intermediate regime. We also find that $\langle K \rangle \sim \langle 1/R_1 \rangle \langle 1/R_2 \rangle \sim 1/L(t)^2$ only in the early regime.

Physical consequences and interpretation of the results.—If we divide the volume V of the system into spheres of radius $L(t)$ connected by the passages we find $\chi(t) \approx Vp(t)/L^3(t)$, where $p(t)$ is the number of necks or passages piercing the surface of the sphere. In the early regime $p(t) \sim 1$ is independent of time indicating that for each sphere of size $L(t)$ we have one passage or connection. In the intermediate regime we find $p(t) \sim t^{1/5}$ indicating the decoupling between domains and connections joining them. The “partially frozen” necks have the local shape of the minimal surface (saddlelike) [10,11] with $H = 0$. They are responsible for slowing down the kinetics and the change of the exponent for the domain growth law from $n = 0.5$ (early regime) to $n = 0.4$ (intermediate regime). The exponent found in the early regime (characterized by the small value of ϕ inside the domains and broad interfaces) follows from the linearized TDGL equation.

Our results do not contradict the late stage scaling hypothesis [1] in the late stages of the phase ordering. In order to prove it we did the simulations for the 2D system of size 1024×1024 and found *three scaling regimes*. The first two regimes are the same as the ones found in the 3D system with the crossover between them

at t_{cr} , and the third regime is the expected late stage scaling regime with $L(t) \sim t^{1/2}$ recovered after quite a long time, $t \geq 400$, not accessible in the 3D system due to the finite size effects even for the system of size $100 \times 100 \times 100$. In the early and intermediate regimes the curvature distribution is peaked at $H = 0$ (with $\langle H \rangle = 0$) in 2D and 3D systems. In 2D it indicates that the system consists of elongated noncircular domains with large parts of flat interfaces. In 3D $H = 0$ and negative $\langle K \rangle$ indicate a saddle shape of the parts of the interface, very characteristic for minimal surfaces [10,11]. The crossover to the late stage scaling regime (with exponent 0.5) occurs in 2D when the domains become “circlelike” with the curvature distribution characterized by a single peak at $H \sim 1/L(t)$ (and not at $H = 0$). The appearance of the preferred nonzero curvature marks the crossover to the late stage scaling regime. This result is important for the application of the Lifshitz-Cahn-Allen argument [5]. Cahn and Allen proved [5] that when the order parameter saturates inside the domains the coarsening proceeds via the local displacement of the interface with the local velocity $v = -H$ irrespective of the dimensionality of the system. The typical time needed to close the domain of size $L(t)$ is $t \sim L(t)/v = L(t)/H_{char}$, where H_{char} is the characteristic curvature in the system. Now if $H_{char} \sim 1/L(t)$ we find $L(t) \sim t^{1/2}$. *In the 3D system we expect the same behavior, i.e., that the crossover from the intermediate to the late stage scaling regime is related to the appearance of the nonzero preferred curvature.* The 3D system is bicontinuous with the single interface separating two \pm percolating domains. This interface should assume the shape of the “constant mean curvaturelike”

surface in the late stage regime. Such surfaces have been studied in the context of periodic surfaces [19].

The late stage scaling has been confirmed in many 2D simulations [20–22]. The intermediate scaling regime in the 2D and 3D systems was observed in Refs. [23–25], but it was incorrectly attributed to the finite size effects [24]. So far late stage scaling has not been confirmed in 3D simulations.

Conclusions.—We have found three scaling regimes in the phase ordering system with two nontrivial crossovers: early-intermediate regime crossover related to the saturation of the order parameter inside the domains and the appearance of partially frozen interface characterized by $H = 0$, and intermediate-late regime crossover related to the appearance of the preferred nonzero curvature [$H \sim 1/L(t)$] of the interfaces between \pm domains.

The morphological studies have been recently done for the spinodal decomposition in 3D systems of homopolymer blends [26,27] and the 2D system of the conserved order parameter [28], but our analysis is the first which provides determination of morphological measures with unprecedented accuracy, giving new insight into phase ordering kinetics.

This work is supported by the KBN Grant No. 2P03B12516. R.H. acknowledges with appreciation the hospitality of Ecole Normale Supérieure, support from the French Ministry of Education, and discussions with Dr. I. Flis-Kabulska.

-
- [1] A. J. Bray, *Adv. Phys.* **43**, 357 (1994).
 - [2] J. S. Langer, in *Solids far from Equilibrium*, edited by G. Godreche (Cambridge University Press, Cambridge, England, 1992), p. 297.
 - [3] K. Binder, *Rep. Prog. Phys.* **50**, 783 (1987).
 - [4] J. D. Gunton, M. San Miguel, and P. Sahni, in *Phase Transitions and Critical Phenomena*, edited by C. Domb and J. L. Lebowitz (Academic Press, New York, 1983), Vol. 8, p. 267.
 - [5] S. M. Allen and J. W. Cahn, *Acta Metall.* **27**, 1085 (1979); I. M. Lifshitz, *Zh. Eksp. Teor. Fiz.* **42**, 1354 (1962).

- [6] Z. W. Lai, G. F. Mazenko, and Oriol T. Valls, *Phys. Rev. B* **37**, 9481 (1988).
- [7] P. Debye, H. R. Anderson, and H. Brumberger, *J. Appl. Phys.* **28**, 679 (1957).
- [8] A. J. Bray and A. D. Rutenberg, *Phys. Rev. E* **49**, R27 (1994).
- [9] P. C. Hohenberg and B. I. Halperin, *Rev. Mod. Phys.* **49**, 435 (1977).
- [10] W. Gózdź and R. Hołyst, *Phys. Rev. Lett.* **76**, 2726 (1996).
- [11] W. Gózdź and R. Hołyst, *Phys. Rev. E* **54**, 5012 (1996).
- [12] T. Ohta, D. Jasnow, and K. Kawasaki, *Phys. Rev. Lett.* **49**, 1223 (1982).
- [13] G. F. Mazenko, *Phys. Rev. Lett.* **63**, 1605 (1989).
- [14] G. F. Mazenko, *Phys. Rev. B* **42**, 4487 (1990).
- [15] A. J. Bray and K. Humayun, *Phys. Rev. E* **48**, R1609 (1993).
- [16] R. E. Blundell, A. J. Bray, and S. Sattler, *Phys. Rev. E* **48**, 2476 (1993).
- [17] C. Yeung, Y. Oono, and A. Shinozaki, *Phys. Rev. E* **49**, 2693 (1994).
- [18] C. L. Emmott, *Phys. Rev. E* **58**, 5508 (1998).
- [19] D. M. Anderson, H. T. Davis, L. E. Scriven, and J. C. C. Nitsche, *Adv. Chem. Phys.* **77**, 337 (1990).
- [20] G. Brown, P. A. Rikvold, and M. Grant, *Phys. Rev. E* **58**, 5501 (1998).
- [21] S. Kumar, J. Vinals, and J. D. Gunton, *Phys. Rev. B* **34**, 1908 (1986).
- [22] G. Brown, P. A. Rikvold, M. Sutton, and M. Grant, *Phys. Rev. E* **56**, 6601 (1997).
- [23] P. S. Sahni and J. D. Gunton, *Phys. Rev. Lett.* **45**, 369 (1980).
- [24] M. K. Phani, J. L. Lebowitz, M. H. Kalos, and O. Penrose, *Phys. Rev. Lett.* **45**, 366 (1980).
- [25] J. D. Shore, M. Holzer, and J. P. Sethna, *Phys. Rev. B* **46**, 11376 (1992); J. G. Amar and F. Family, *Bull. Am. Phys. Soc.* **34**, 491 (1989).
- [26] H. Jinnai, T. Koga, Y. Nishikawa, T. Hashimoto, and S. T. Hyde, *Phys. Rev. Lett.* **78**, 2248 (1997); H. Jinnai, Y. Nishikawa, and T. Hashimoto, *Phys. Rev. E* **59**, R2554 (1999).
- [27] A. Aksimentiev, K. Moorthi, and R. Hołyst, *J. Chem. Phys.* **112**, 6049 (2000).
- [28] K. R. Mecke and V. Sofonea, *Phys. Rev. E* **56**, R3761 (1997); V. Sofonea and K. R. Mecke, *Eur. Phys. J. B* **8**, 99 (1999).